SANDIA REPORT

SAND2004-2289
Unlimited Release
Printed July 2004

Inspection Strategy for LIGA Microstructures Using a Programmable Optical Microscope

Joseph T. Ceremuga, Georg Aigeldinger

Prepared by Sandia National Laboratories
Albuquerque, New Mexico 87185 and Livermore, California 94550

Sandia is a multiprogram laboratory operated by Sandia Corporation,
a Lockheed Martin Company, for the United States Department of Energy's
National Nuclear Security Administration under Contract DE-AC04-94AL85000.

Issued by Sandia National Laboratories, operated for the United States Department of Energy by Sandia Corporation.

Available to DOE and DOE contractors from
U.S. Department of Energy
Office of Scientific and Technical Information
P.O. Box 62
Oak Ridge, TN 37831

Telephone: (865)576-8401
Facsimile: (865)576-5728
E-Mail: reports@adonis.osti.gov
Online ordering: http://www.osti.gov/bridge

Available to the public from
U.S. Department of Commerce
National Technical Information Service
5285 Port Royal Rd
Springfield, VA 22161

Telephone: (800)553-6847
Facsimile: (703)605-6900
E-Mail: orders@ntis.fedworld.gov
Online order: http://www.ntis.gov/help/ordermethods.asp?loc=7-4-0#online

SAND2004-2289
Unlimited Distribution

Inspection Strategy for LIGA Microstructures Using a Programmable Optical Microscope

Joseph T. Ceremuga and Georg Aigeldinger
Sandia National Laboratories
7011 East Avenue, MS9401
Livermore, California 94550 USA

Thomas R. Kurfess
Woodruff School of Mechanical Engineering
Georgia Institute of Technology
813 Ferst Drive
Atlanta, Georgia 30332 USA

Abstract

The LIGA process has the ability to fabricate very precise, high aspect ratio mesoscale structures with microscale features [1]. The process consists of multiple steps before a final part is produced. Materials native to the LIGA process include metals and photoresists. These structures are routinely measured for quality control and process improvement. However, metrology of LIGA structures is challenging because of their high aspect ratio and edge topography. For the scale of LIGA structures, a programmable optical microscope is well suited for lateral (XY) critical dimension measurements [2]. Using grayscale gradient image processing with sub-pixel interpolation, edges are detected and measurements are performed [3]. As with any measurement, understanding measurement uncertainty is necessary so that appropriate conclusions are drawn from the data. Therefore, the abilities of the inspection tool and the obstacles presented by the structures under inspection should be well understood so that precision may be quantified. This report presents an inspection method for LIGA microstructures including a comprehensive assessment of the uncertainty for each inspection scenario.

THIS PAGE INTENTIONALLY LEFT BLANK

TABLE OF CONTENTS

THIS PAGE INTENTIONALLY LEFT BLANK

Inspection Strategy for LIGA Microstructures Using a Programmable Optical Microscope

1. Introduction

The LIGA process uses deep X-ray lithography and electroforming to create high aspect ratio microstructures. This technology is well established at Sandia National Laboratories (SNL) and other institutions worldwide [1, 4]. Dimensional metrology for these microparts is crucial for process control and to assure dimensional control. However, the edge topography, high aspect ratio geometry, and material type make metrology of LIGA parts a challenging task, with much room for improvement [5]. Often design specifications require better than +/-5% tolerance for meso- and micro-scale features, thus test accuracy is a concern. Test accuracy refers to the uncertainty of the measurement tool with respect to the tolerances of the characteristics being measured [6]. A suitable test accuracy of 25% [6] leaves little room for uncertainty during inspection. For example, a 150 μm feature may have a tolerance specification of +/-5 μm (+/-3.3% of the feature size). The uncertainty in measuring this feature must be less than or equal to +/-1.25 μm to meet the required test accuracy. This work addresses the uncertainty issues that high aspect ratio mesoscale structures with microscale features present in non-contact, non-destructive dimensional metrology using a programmable optical microscope. Inspection quality of this type is dependent on what the camera senses, as well as what the edge detection algorithms are able to decipher. While the manufacturer specifies submicron resolution and accuracy [3], this level of inspection may be difficult to achieve for LIGA structures.

Another challenge is that calibration standards for optical gauging microscopes are generally composed of thin chrome on glass, having virtually no thickness (~0.1 μm anti-reflective chrome) and no topology compared to LIGA structures. Objects of this type require straightforward illumination characteristics for accurate inspection, and are used to properly assess the attainable precision of the optics as well as the stage accuracy of this tool. In contrast, structures composed of materials native to SNL's LIGA process, such as negative and positive photoresists, and electrodeposited metals, require distinctive light type and light intensity settings for proper inspection.

These two settings are crucial to obtain suitable contrast in an image for edge detection, ensuring an accurate measurement. Adjusting the intensity is straightforward: one should use enough light to achieve contrast, yet avoid flooding the sensor so that image saturation or "blooming" does not occur. A study on how edge detection is affected by a

change in light type and intensity is performed in this research on chrome and high aspect ratio LIGA specimens.

The optical microscope suits the inspection scale desired for LIGA metrology very well [2]. The microscope used in this study is a VIEW Engineering Voyager V6x12 [3]. The hardware and the software of this tool are commercially available, and are used as supplied by the vendor.

2. LIGA

The LIGA process was developed in the early nineteen-eighties at Research Center Karlsruhe, Germany, in an effort to precisely fabricate microscopic nozzles for the separation of uranium isotopes [7]. LIGA is a German acronym for lithography (Lithographie), electrodeposition (Galvanoformung), and molding (Abformung).

To produce parts using LIGA, an X-ray mask must be produced. At SNL, the computer aided design is transferred to a chrome-on-glass UV-lithography mask using a commercial patterning process [7]. To create the X-ray mask, positive or negative photoresist (e.g. Novolac or SU8) is spun on a thin mask membrane. The mask blank is exposed and developed. Then the open regions are filled with gold to absorb the X-rays [8].

The mask is then placed in front of a sheet of PMMA (bonded to a silicon wafer) and exposed to X-rays. Because a very high dose is required for thick PMMA, LIGA facilities are located at synchrotron storage ring facilities such as ALS (Advanced Light Source) at Lawrence Berkeley National Laboratories, SSRL (Stanford Synchrotron Radiation Laboratory) at Stanford University, APS (Advanced Photon Source) at Argonne National Laboratories, CAMD (Center for Advanced Microstructures and Devices) at Louisiana State University, and NSLS (National Synchrotron Light Source) at Brookhaven National Laboratories.

During exposure, main chain scission of the PMMA polymer reduces the mean molecular weight by two orders of magnitude. Using an organic development bath, the exposed areas of the PMMA are dissolved [7]. Surface roughness characteristics of the sidewalls can be of optical quality, reported to have average roughness values < 50 nm [9]. Sidewall normality depends upon mask and beam alignment during exposure, secondary radiation effects, and the material characteristics of the mold [7].

Metal is electrodeposited into the PMMA mold onto a thin, conductive copper "seed" layer that is plated on the silicon substrate. This result in either a mold for future use in injection molding or direct LIGA parts once removed from the substrate. This research deals with the inspection of direct LIGA parts, made from nickel and nickel alloys.

To produce released LIGA microstructures, the PMMA mold is overplated to ensure that the entire mold is filled to the top. Lapping and polishing procedures planarize and polish the top surface, removing PMMA and the nickel overplating, to achieve part thickness specifications. The PMMA is then dissolved from the substrate leaving only the bare electroplated parts. The parts are released by dissolving a thin copper layer between the parts and the substrate.

LIGA has been considered a technology that bridges the gap between silicon microfabrication and classical high precision machining. This technology provides an elegant solution for creating two-and-a-half dimensional (two-dimensional with a thickness) meso- and micro-scale structures with unprecedented aspect ratios and precision [8]. The ability to use the structures as a mold for casting offers much potential for commercial applications, having faster reproduction times than the lithography step [7]. Materials available for final LIGA parts are electrodeposited metals as well as all those used in molding processes such as plastics, ceramics, etc. Present LIGA metrology methods lack the precision to properly quantify the limits of LIGA microfabrication. For process control and improvement, the development of robust metrology methods for LIGA microstructures is required.

3. Experimental Setup

The most common features encountered in LIGA fabrication are channels and lines. Therefore, a chrome pitch standard was chosen as the first specimen to be examined. The standard is patterned with pitches varying from 2 μm to 500 μm in size certified +/-0.26 μm. By using a chrome specimen, ideal for edge detection, the microscope's ability to measure a linewidth or pitch may be assessed.

The experiment consists of selecting a range of light intensities for each light type offered by the microscope. Figure 1 shows a principle sketch of the microscope and its available lighting options.

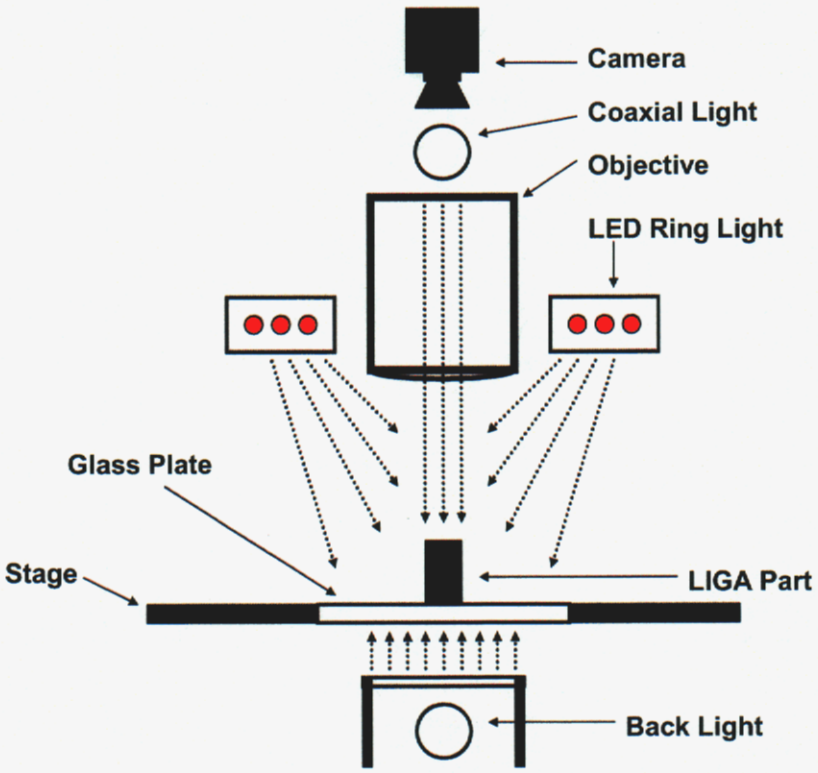

Figure 1: Principle sketch of microscope setup

The intensity ranges were chosen so that the resulting image had enough contrast for the edge detection algorithm to execute properly. Measurements were taken so that the extents of the feature were within the field of view of the camera during inspection so that no stage movement was necessary, eliminating uncertainty contributed by the stage movement. Pitches of 50μm, 100 μm, 150 μm, and 200 μm in size were measured. Light intensity was varied from 19% to maximum intensity, in 5% increments. Ten

measurements were taken at each intensity. Since coaxial (top) lighting was unable to produce acceptable contrast, only back lighting and LED ring lighting were used on the chrome standard. Figure 2 shows the results of these measurements for the 50 μm pitch.

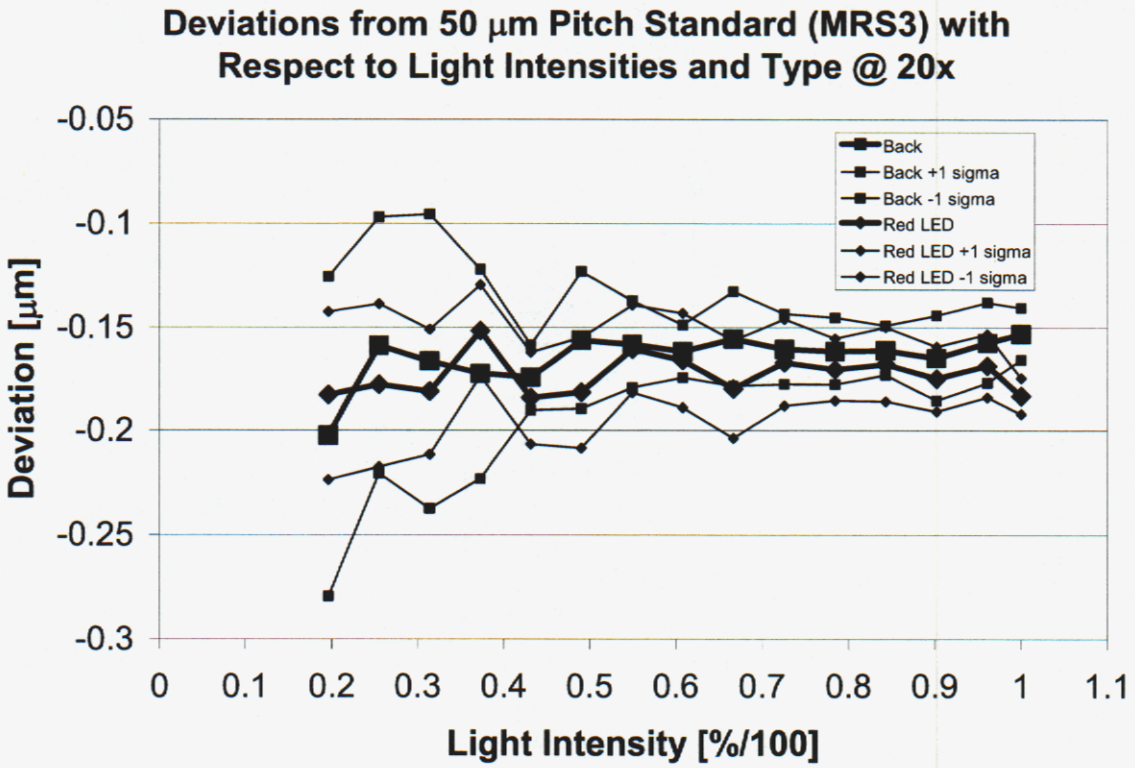

Figure 2: Light intensity study results from the chrome pitch standard

As shown in Figure 2 the thicker lines represent the mean values of the ten measurements taken at the specified light intensity. The standard deviations (thin lines in Figure 2) show that as the light intensity reaches about 50% of the maximum, the measurements become more consistent. Therefore, it can be seen that a setting above 50% is required for best reproducibility. The results of averaging these values are in Table 1. The results show little difference in the measurements with respect to the choice of light type.

Table 1: Chrome pitch specimen results: Deviation from 50 μm certified measurement (Back Light and LED Ring Light: 50% - 100%)

Light Type	Mean Deviation +/-σ [μm]
Back Light	-0.16 +/-0.02
LED Ring	-0.17 +/-0.02

This difference between the two light types is insignificant because a pitch measurement is not affected by light types. However, changes in light type will have an effect on linewidth measurements. This is best understood by the grayscale intensity profile of the image during inspection. The intensity profile is governed by the image contrast and the image sharpness of the edge of a specimen. The image contrast is dependent on the reflectivity of the specimen within the field of view and the intensity of light used to illuminate it. Other parameters that affect image contrast are modulation transfer and optical transfer, but these topics are beyond the scope of this report.

The difference between a pitch and a linewidth is illustrated in Figure 3. The upper portion of the diagram shows a grayscale principle sketch from the camera of the microscope with edge finders, and the bottom portion plots grayscale intensity profiles with respect to the dotted line on each feature.

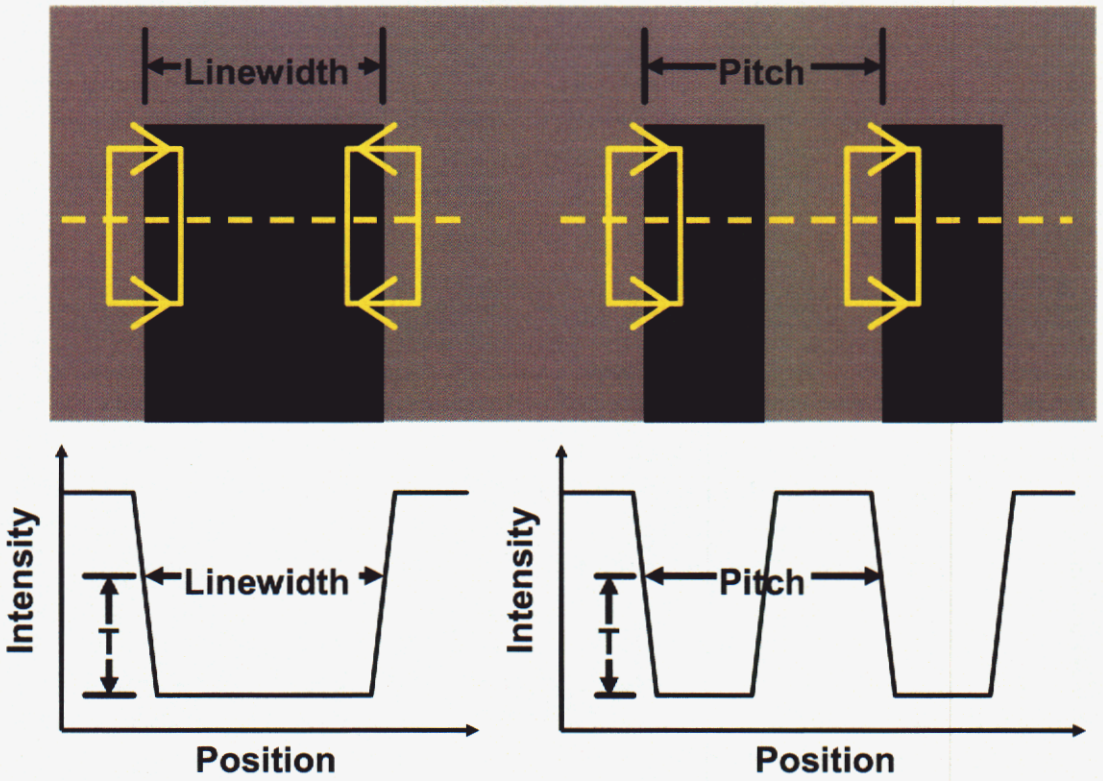

Figure 3: Principle linewidth and pitch diagrams with image intensity profiles

Therefore, the difference in measurement between a linewidth and pitch is dependent on the intensity threshold T (Figure 3) at which the image processing software defines an edge [10]. Regardless of how the intensity threshold is defined in the edge detection algorithm, the pitch will remain the same size across similar edge intensity profiles. This is not the case for linewidths. By looking at the image intensity profiles in Figure 3, if the intensity threshold T were to change, the linewidth measurement would change whereas the pitch measurement would remain. To show that the linewidth measurement is affected by different light types, a similar lighting test was performed on a 25 µm linewidth. This feature was not a certified width, but for this test, it does not have to be, since relative values are of interest, rather than the absolute values. The light intensity increased from 50% in 5% increments until maximum light intensity was reached for both the back light and LED ring light. Figure 4 shows the mean deviation (from the nominal 25 µm) for the two lighting types across the intensity range.

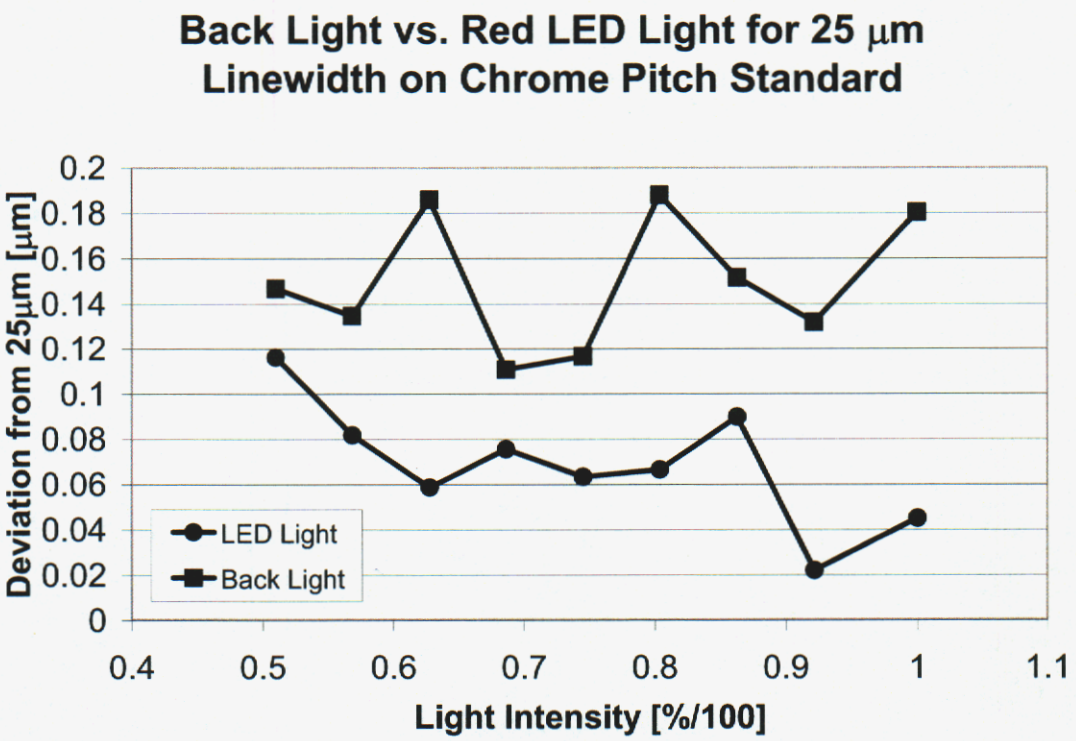

Figure 4: Linewidth measurements across intensities for back and LED ring lighting.

Table 2 shows the results of this linewidth test.

Table 2: Chrome linewidth specimen results: Deviation from 25 μm nominal linewidth (Back light and LED ring light: 50% - 100%)

Light Type	Mean Deviation +/-σ [μm]
Back Light	0.16 +/-0.09
LED Ring	0.07 +/-0.10

This experiment has shown that linewidth measurements are dependent on light type and intensity.

4. Measuring Released Metal Parts

To simulate a final LIGA part, a 150 μm NIST traceable stainless steel gauge block (certified to +/- 0.04 μm) was encased in clear epoxy polymer and then planarized by lapping and polishing procedures (as used in our baseline LIGA process). Following planarization, final length, width, and height dimensions were 30 mm, 0.150 mm, and 6.752 mm, respectively. After dissolving the epoxy from the specimen, the 150 μm width measurement was taken using a similar range of light intensities and lighting types offered by the microscope used for the chrome standard testing. The coaxial light was added to this study, taking measurements across a larger intensity range. Figure 5 shows images from the microscope of the gauge block using each type of light through the 20x objective lens.

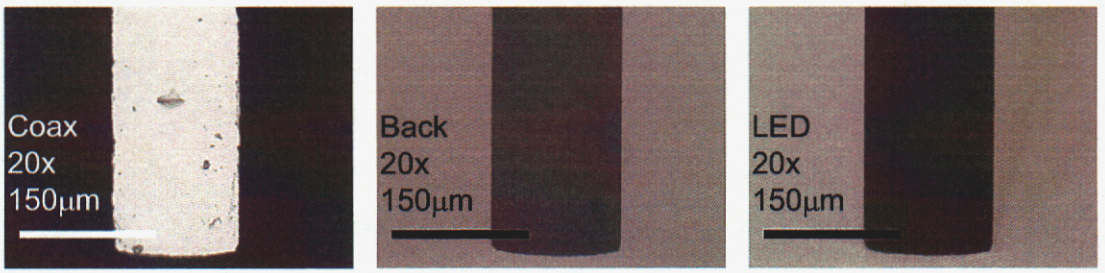

Figure 5: Images of gauge block using the 20x objective under coaxial, back, and LED ring lighting conditions (arbitrary intensities).

A visual comparison between back light and LED ring light images reveals no distinguishable difference with respect to the more correct lighting condition. Inspecting the gauge block with the 10x objective shows which light type facilitates the more correct measurement. Figure 6 shows images using each light type with the 10x objective.

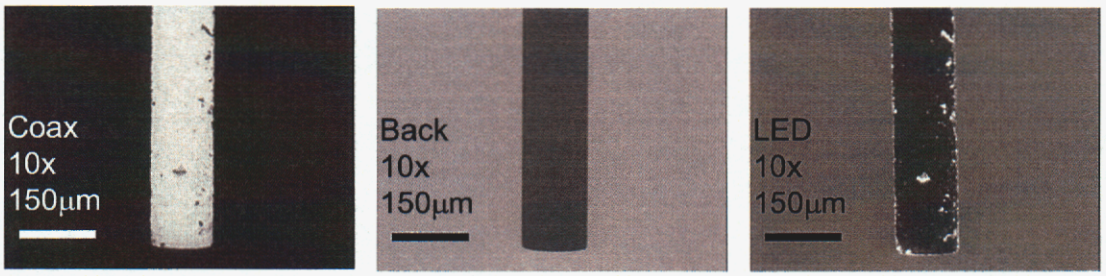

Figure 6: Images of gauge block using the 10x objective under coaxial, back, and LED ring lighting conditions (arbitrary intensities).

Using the 10x objective, the surface roughness is more pronounced under the LED ring light as seen when using the coaxial light. The light intensity test was performed, and the measurement results using 10x and 20x objectives are shown in Figure 7.

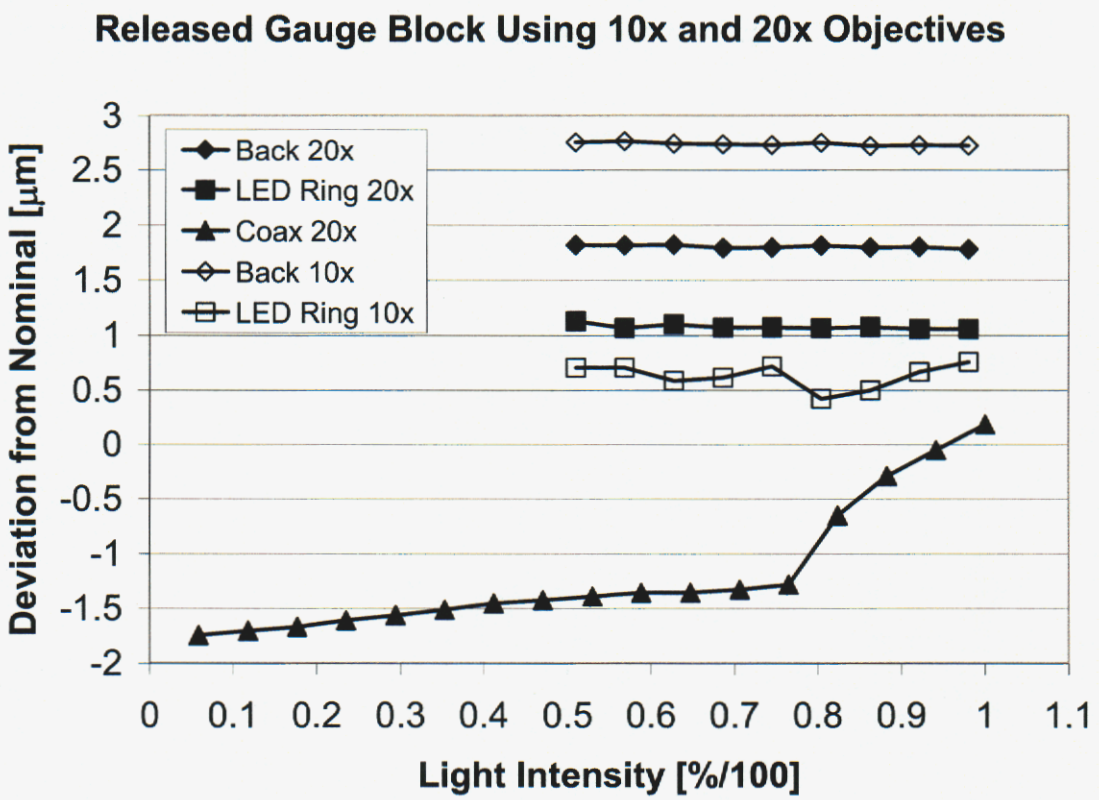

Figure 7: Light intensity study comparison of results using 10x and 20x objectives.

First of all, there is a much larger difference (0.72 μm) between the back light and the LED ring light measurement in comparison to the chrome specimen (0.09 μm) when using the 20x objective. This variation may be attributed to the high aspect ratio of the structure as well as the edge topology. Standard deviations exhibit the same trends for light intensities below 50%. Deviations seen in Figure 7 beyond the specified precision of the certified gauge block are due to altering the gauge block by lapping and polishing processes [11].

The image of the gauge block under the coaxial light shows that edge topology significantly skews the measurement, illustrated in Figure 7.

The results show that the measurements taken with the 10x objective exhibit more variation than the other data sets. The graph shows that both the 10x and 20x measurements, when using the backlight, are larger than their LED ring-illuminated counterparts. The 20x data is enveloped by the 10x data, suggesting a more accurate measurement resulting from the higher resolution of the 20x lens. Table 3 shows the results from this lighting test.

Table 3: Deviations from 150 μm for the released gauge block across light types and objectives

Objective	Back Light: Mean +/-σ [μm]	LED Ring Light: Mean +/-σ [μm]
20x	1.80 +/-0.06	1.09 +/-0.06
10x	2.75 +/-0.05	0.58 +/-0.49

The outlier in the results is the standard deviation of the LED ring light measurements at 10x magnification. This demonstrates that the measurement is less consistent for parts with surface/edge topography when using the ring light. At higher magnification, this inconsistency is not recognizable in the video, yet present in the measurement. Therefore, to achieve the least uncertain measurement, use of the back light is recommended for released metallic parts and chrome masks.

5. Measuring Patterned Photoresist

The gauge block aids in understanding the final "released part" step in direct LIGA. However, in order to aid process improvement through metrology, all of the steps in the production process must be examined. These steps involve structures of SU8 and PMMA, negative and positive photoresists, respectively [8]. In the SNL LIGA process both of these materials are patterned transparent polymers bonded to highly reflective metal films on a polished substrate. This combination of materials, combined with a finite radius at the top edge of the structure, results in a dark line that represents the edge of the structure in the microscope image. Figure 8 shows microscope images of both polymers under inspection.

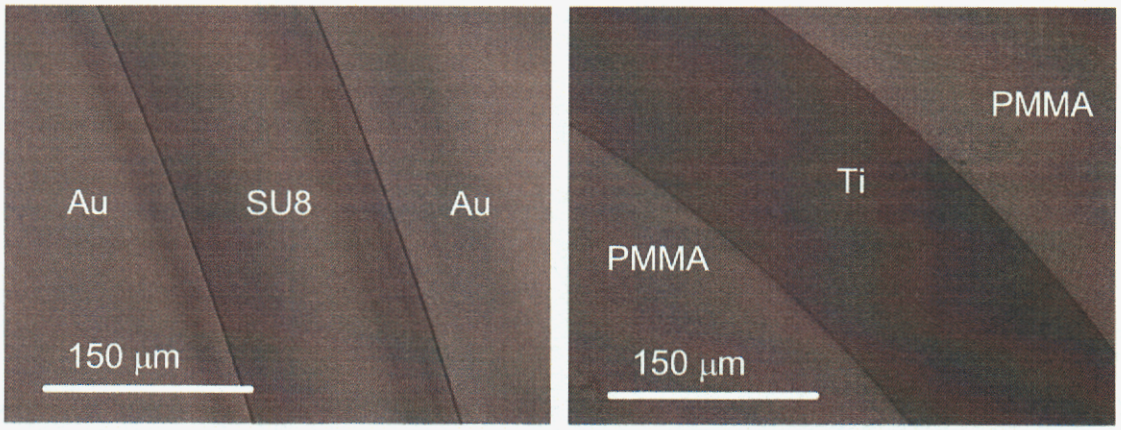

Figure 8: SU8 on gold and PMMA on titanium; both imaged with the 20x objective.

Photoresist structures are either the negative or positive tone of the design. The simplest approach for inspection would be to measure the outermost edge of either the SU8 or PMMA structure. However, the rounded edge of the structure poses problems for image processing. The outermost edge in the image is located where the rounded edge meets with the sidewall of the structure. The steep vertical makeup at this location produces a vignetting effect in the image at the edge of the structure. Thus, a low-contrast transition makes the gradient grayscale edge-detection difficult, and in some cases unobtainable, depending on material reflectivity and structure sizes within the field of view. In addition, the photoresist/material-side of the dark line is always present with acceptable contrast for consistent edge detection. The high contrast is due to focusing the lens on a surface and not a sidewall, from an overhead perspective. The depths of focus of the objectives are on the order of a micron. Figure 9 shows an image where the dark line is present, showing low-contrast on the void-side and high-contrast on the material side. Figure 9 also has a labeled cross-section of the image as a principle sketch for clarification.

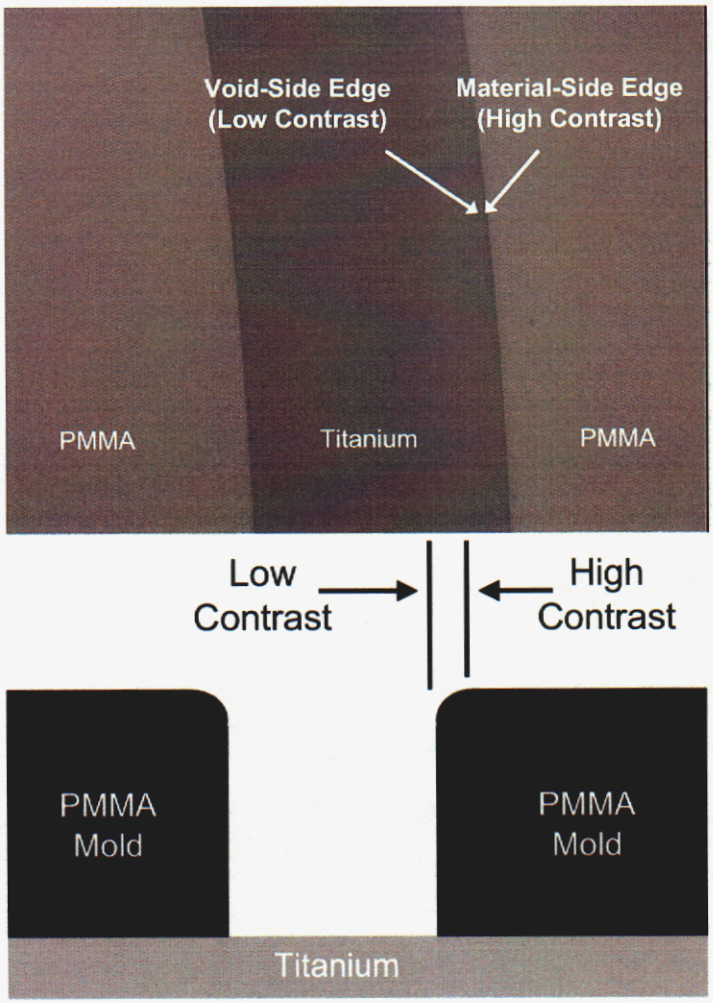

Figure 9: Video image and principle sketch.

Since consistency is necessary in metrology, the high-contrast, material-side edge is the more desirable edge to inspect. However, to account for the representative width of the dark line in the image, the dark line must be measured in locations across the wafer/specimen where it is available with acceptable contrast on both sides. The width of the dark line depends on the depth of focus of the lens and the amount of topology on the edge (~2 μm fillet radius). Typically, using the 20x objective, the width of the dark line is approximately 2 μm and varies with a standard deviation of +/-0.3 μm, calculated from a data set of ten measurements from a sample wafer.

Once an average and standard deviation of the width is known, the high contrast, material-side measurement can be corrected according to the structure being measured.

Figure 10 shows inspected and corrected linewidth and channel measurements for SU8 masks and PMMA molds, respectively.

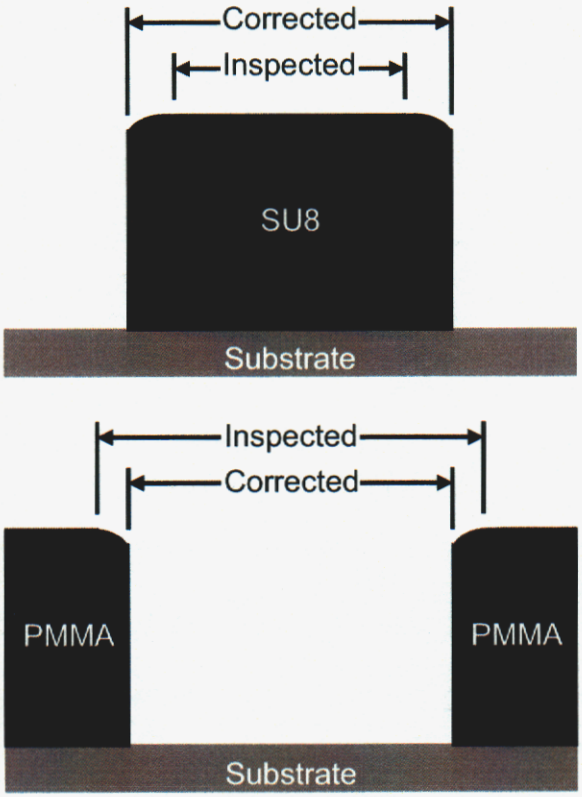

Figure 10: Principle sketch of photoresist correction for linewidth and channel measurements

The correction involves adding/subtracting twice the width of the dark line, since two edges are encountered, in the linewidth/channel measurement. The standard deviation is used in the uncertainty analysis of the inspection scenario explained later in this report.

To understand the effect that light intensity has on the photoresist measurement, the lighting test was performed using only the coaxial light with both 10x and 20x objectives. The LED ring light is not an effective illumination option for inspecting transparent photoresists on highly reflective metallized wafers. The image contrast produced by this light is not suitable for edge detection. Results for the coaxial light measurements are shown in Figure 11.

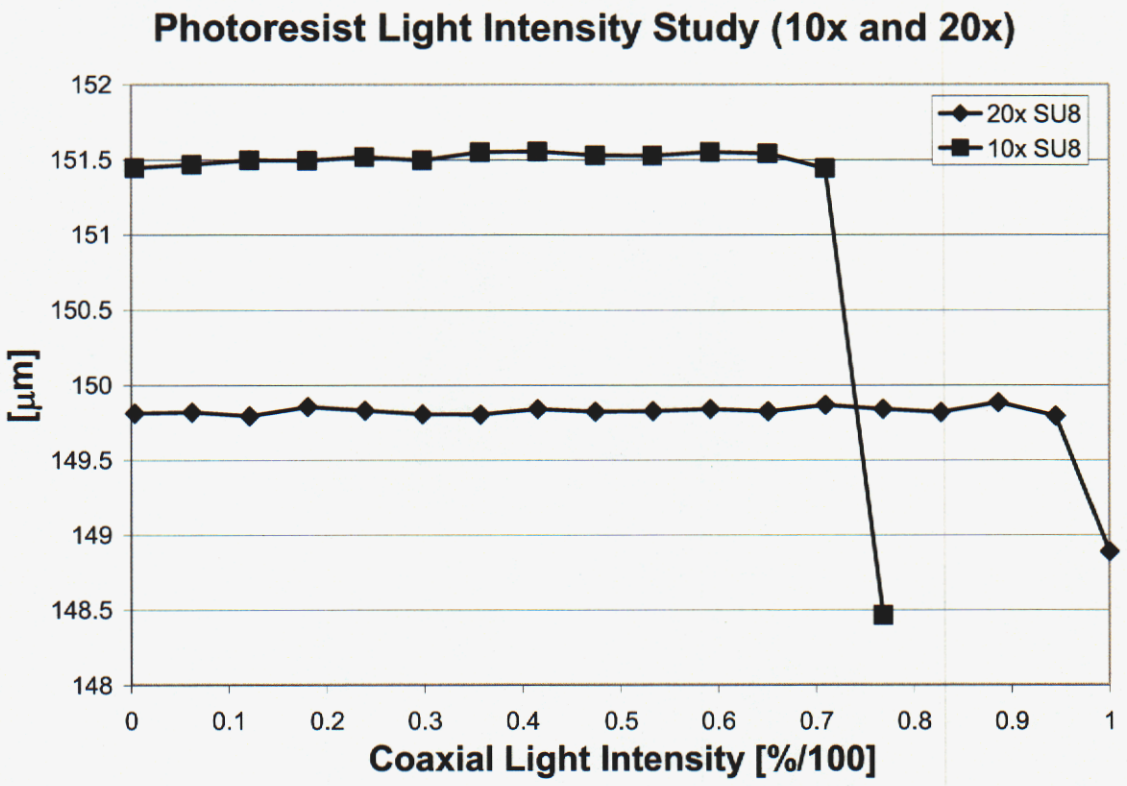

Figure 11: Light intensity study performed on 150 µm SU8 linewidth using the10x and 20x objectives

Across the range of the light intensity, measurements remain consistent until a noticeable drop indicates light saturation of the sensor. By the results shown, as long as there is sufficient contrast in the image so that edge detection may be performed, and light saturation is avoided, the measurement will not vary outside the repeatability of the microscope across the available light intensity range. Table 4 shows the mean and standard deviation from the study.

Table 4: Coaxial light intensity test results: 150 µm PMMA photoresist channel

Objective	Mean +/-σ [µm] (intensity)
20x	149.83 +/-0.02 (1%-95%)
10x	151.51 +/-0.04 (1%-70%)

6. Determining Uncertainty in the Measurements

The main purpose for studying the optical inspection of the various structures of the LIGA process is to assess the amount of uncertainty in each measurement. A single value that covers the inspection uncertainty for all LIGA metrology situations is not an effective option. As explored, many factors contribute to the uncertainty in each measurement. The measurement uncertainty for each inspection scenario is calculated as a combined standard uncertainty using a root sum-squared (RSS) method shown in Equation 1 [12, 13].

$$U_{inspection} = \sqrt{U_1^2 + U_2^2 + \ldots + U_n^2} \tag{1}$$

Information obtained from earlier studies surveyed the capabilities of the instrument, quantified uncertainty in the stage, optics, and measurement repeatability [14]. Table 5 shows the possible uncertainty contributions for measuring LIGA structures.

Table 5: Uncertainty components of LIGA metrology

Uncertainty Component	Value
U_{optics}	1μm (chrome calibration standard)
U_{stage}	3.69μm (95% confidence)
$U_{repeatability}$	0.14μm (95% confidence)
$U_{released\ parts}$	0 (as if measuring a chrome part)
$U_{photoresist}$	σ_{edge} (after bias for material-side inspection)
$U_{back\ lighting}$	0.1μm
$U_{LED\ ring\ lighting}$	0.1μm
$U_{coaxial\ lighting}$	0.1μm
$U_{temperature}$	Length/Material dependent
$U_{lapping/polishing}$	Must be characterized by optical profiler or SEM

The uncertainty in the certified chrome calibration standard determines the uncertainty in the optics. The stage uncertainty was found using a high resolution grid plate taking the RSS value using the maximum mean positional deviation and twice (95% confidence) the maximum standard deviation. The repeatability was calculated by twice the average standard deviation of an arbitrary test that measured the same feature multiple times. After understanding that using the back light defines the correct edge for chrome and released metal structures, the uncertainty contribution from this material type is covered by that of the calibration standard for the optics. When inspecting photoresist structures,

the standard deviation calculated from numerous dark line width measurements is the uncertainty component.

Understanding the uncertainty in each individual light source throughout its intensity range is necessary for data comparison. Measurements taken with the same light type at different intensities can be compared since the effect that a variation in light intensity has on the measurement has been examined. These components were calculated by the range of the mean inspection values across the intensities during the lighting tests. For instance, if a released part was inspected once with 50% back lighting and then again using 75% backlighting, the measurements may vary by 0.1 μm. It is difficult to evaluate this level of uncertainty because it nears the repeatability of the microscope.

Variations in temperature may also contribute to measurement uncertainties. The measurement uncertainty associated with temperature depends on the material properties as well as the size of the specimen. For example, a 500 μm photoresist linewidth structure, having the largest coefficient of thermal expansion of the LIGA materials (70 μm/m·K), would expand 0.07 μm (0.035 μm per edge) if exposed to two degrees of temperature change. Performing measurements across large distances will have greater impact on the uncertainty due to temperature fluctuations. The temperature in the metrology lab is monitored and was found to vary by +/-1 °C of variation, which is acceptable for IC metrology labs [15]. The following is an example of inspection and uncertainty assessment for a PMMA mold feature.

7. Example of Measurement Uncertainty: 150 µm Channel of a PMMA Mold

Calculating the inspection uncertainty of the linewidth measurements for 150 µm channels in a PMMA mold involves several steps. After choosing the 20x objective, the width of the dark line at the structure's edge is inspected at several locations where it is available. The mean and standard deviation of this data is then calculated. Next, the inspection program is set up to capture the material side of the dark line that represents the edge of the PMMA. Coaxial light intensity was set between 1% and 95% to produce acceptable contrast. After completing the inspection routine, the linewidth measurements were corrected and the inspection uncertainty was calculated. In the structures examined, the PMMA that surrounds the 150 µm channel is approximately 700 µm wide before the next channel is encountered. In a simplified scenario, the thermal expansion occurring at the top surface of the structure is considered uniform across the 700 µm width although the PMMA is fixed to the metallized wafer. The room was at 23.8 +/-1 °C during inspection. The coefficient of thermal expansion of the PMMA is 70 µm/m·K and is applied to the variability of the temperature control of the room. The summary of all uncertainties for this PMMA mold inspection is given in Table 6.

Table 6: PMMA channel inspection and uncertainty data

Inspection Data	Value [µm]
Edge Width (10 samples)	2.03 +/-0.48 (95% confidence)
Linewidth Data (20 samples)	156.45 +/-2.80 (95% confidence)
Adjusted Linewidth Data (bias = -4.06µm)	152.39 +/-2.80 (95% confidence)
U_{optics}	+/-1 (chrome calibration standard)
$U_{repeatability}$	+/-0.14 (95% confidence)
$U_{photoresist}$	+/-0.68 (95% confidence for two edges)
U_{stage}	0 (FOV measurement)
$U_{coaxial\ lighting}$	0 (no data to compare to)
$U_{temperature}$	+/-0.49 (from +/-1 degree Celsius)
$U_{lapping/polishing}$	0 (none performed)

Therefore, calculating the combined standard uncertainty of the four contributing components (optics, repeatability, photoresist, and temperature), the PMMA mold inspection has an inspection uncertainty of +/-1.31 µm at 95% (2σ) confidence associated with the adjusted linewidth data. The uncertainty components that were not used in this example should be incorporated for cases dealing with non-FOV measurements, comparisons between data sets taken at different light intensities (using the same light type), and metal structures that undergo lapping and polishing procedures.

8. Uncertainty Limitations

The scenario presented in the previous section assessed measurement uncertainty from four sources. To minimize the amount of uncertainty, each contributor must be examined. The major contributor was the one-micron uncertainty in the optics. This value is based on the certification of the standard. The simplest way to improve this number is to calibrate the optics with a more accurate standard. Although stage uncertainty was not included in the PMMA channel example the same idea is applied to improving stage uncertainty; a more accurate stage calibration standard reduces the uncertainty component contributed by the stage. The uncertainty due to the PMMA mold edge is the second major contributor. Improvements in this uncertainty would result from optimization of the LIGA process. The uncertainty from temperature change is related to the overall temperature change throughout the duration of the inspection. Improved temperature control of the room, ensuring lesser than +/-2 °C temperature change or less, reduces this uncertainty. Finally, repeatability is dependent on the architecture of the microscope and would require equipment upgrades (hardware/software) to reduce uncertainties.

9. Conclusions

The study was performed to develop a process to make metrology data acquisition more reliable and accurate. We achieved this by performing a critical analysis of limitations and uncertainties on our laboratory, the programmable optical microscope, and LIGA process characteristics. By implementing this inspection strategy, a better understanding of the precision of the microscope and the nuances of inspecting high aspect ratio microstructures is obtained. This gives greater confidence in the accuracy of inspection results generated by the programmable optical microscope for inspection scenarios that may be encountered in the LIGA process. LIGA technology benefits from precise inspections throughout all process steps so that further post-processing and process improvement decisions may be made based on robust metrology data. This research necessitates the need for ongoing metrology development and customization for high-precision manufacturing processes through an in-depth investigation of LIGA microfabrication.

10. References

[1] Becker EW, et al. Fabrication of Microstructures with High Aspect Ratios and Great Structural Heights by Synchrotron Radiation Lithography, Galvanoforming, and Plastic Moulding (LIGA Process). Microelectronic Engineering 1986; 4:35-53.

[2] Bono MJ, Hibbard R, Meso-scale Metrology Tools: A Survey of Relevant Tools and a Discussion of Their Strengths and Weaknesses. ASPE Proceedings 2003: Winter Topical Meeting, Gainesville, USA, 2003. pp 70-73.

[3] VIEW Engineering (http://www.vieweng.com).

[4] Hruby J, LIGA Technologies and Applications. MRS Bulletin 2001; 26(4); 337-340

[5] Dewa AS, Mesoscopic Systems: Bridging from Micromachined Devices to Macroscopic Systems. Mechatronics 1998; 8(5); 521-534.

[6] Davis, McNabb, Taylor R, Ruth FD. General Workmanship Requirement 9900000, Albuquerque, 2001

[7] Menz W, Mohr J, Paul O. Microsystem Technology, 1st Edition, New York: John Wiley and Sons, 2001.

[8] Madou M. Fundamentals of Microfabrication. Boca Raton: CRC Press, 1997.

[9] Hecht E. Optics, San Francisco: Addison Wesley, 2002.

[10] Vezzetti CF, Varner RN, et al. Bright-Chromium Linewidth Standard, SRM 476, for Calibration of Optical Microscope Linewidth Measuring Systems. Gaithersburg, the National Institute of Standards and Technology, 1991.

[11] Aigeldinger G, Ceremuga J, and Skala D. Large Batch Dimensional Metrology Demonstrated in the Example of a LIGA Fabricated Spring. Book of Abstracts, HARMST 2003, Monterey, USA 2003. pp 263-264.

[12] NIST. Guidelines for Evaluating and Expressing the Uncertainty of NIST Measurement Results, NIST Technical Note 1297. Gaithersburg, the National Institute of Standards and Technology, 1994.

[13] NIST. Physical Reference Data (http://physics.nist.gov/cuu/). Gaithersburg, the National Institute of Standards and Technology, 2003.

[14] Ceremuga J. Optimizing Inspection of High Aspect Ratio Microstructures Using a Programmable Optical Microscope. Atlanta, the Georgia Institute of Technology, 2003.

[15] Integrated Circuit Engineering Corporation. Practical Integrated Circuit Fabrication Seminar. Scottsdale, 1998; 16; pp 14.

DISTRIBUTION:

4 Institut fur Mikrostrukturtechnik
Attn: V. Saile
J. Mohr
F. J. Pantenburg
P. Meyer
Forschungszentrum Karlsruhe
Hermann-von-Helmholtz-Platz 1
76344 Eggenstein-Leopoldshafen
GERMANY

1 Osservatorio Astronomico di Brera
Attn: M. Ghigo
Via E. Bianchi 46,
23807 Merate (LC)
ITALY

4 Honeywell Federal Manufacturing & Technologies
Attn: Robert G. Steinhoff
Sherri Huffman
Madhuri Widmar
B. L. Dearth
PO Box 419159
Kansas City, MO 64141

2 Center for Advanced Microstructures and Devices
Attn: J. Goettert
Y. Desta
6980 Jefferson Highway
Baton Rouge, LA 70803

1 Georgia Institute of Technology
Attn: Thomas R. Kurfess
MARC 435
813 Ferst Drive N.W.
Atlanta, GA 30332

1 U.S. Department of Energy
Attn: Craig C. Henderson
NA-115/Forrestal Building
1000 Independence Avenue, SW
Washington, DC 20585

1 MS0196 R. Wild, 2618
1 MS0319 J. R. Fellerhoff, 2610

1	MS0319	D. E. Petersen, 2618
1	MS0319	C. W. Vanecek, 2618
1	MS0437	C.L. Knapp, 2120
1	MS0437	J. M. McGlaun, 2830
1	MS0503	D.W. Plummer 2330
1	MS0561	T. T. Smith 14111
1	MS0889	S. V. Prasad, 1851
1	MS0958	G. L. Benavides 14184
1	MS0958	E. A. Bryce, 14133
1	MS1007	J. Jones, 15272
1	MS1007	L. Shipers, 15272
1	MS1310	S. N. Kempka, 9113
1	MS1310	M. A. Polosky, 2614
1	MS9001	M. E. John, 8000; Attn:
	MS9004	R. H. Stulen, 8100
	MS9007	D. R. Henson, 8200
	MS9054	W. J. McLean, 8300
	MS9002	P. N. Smith, 8500
	MS9003	K. E. Washington, 8900
1	MS9005	B. K. Damkroger, 8240
1	MS9036	M. A. Forman, 8245
1	MS9161	W. R. Even, 8760
1	MS9403	J. M. Hruby, 8700
1	MS9404	G. D. Kubiak, 8750
1	MS9401	J. E. M. Goldsmith, 8751
1	MS9401	M. A. Hekmaty, 8751
1	MS9401	L. L. Hunter, 8751
1	MS9401	K. D. Krenz, 8751
1	MS9401	M. E. Malinowski, 8751
1	MS9401	S. Mrowka, 8751
1	MS9401	D. M. Skala, 8751
1	MS9401	A. A. Talin, 8751
15	MS9401	G. Aigeldinger, 8753
1	MS9401	D. R. Boehme, 8753
1	MS9401	G. F. Cardinale, 8753
15	MS9401	J. T. Ceremuga, 8753
1	MS9401	J. T. Hachman, 8753
1	MS9401	J. J. Kelly, 8753
1	MS9401	D. E. McLean, 8753
1	MS9401	T. I. Wallow, 8753
1	MS9401	P. C. Y. Yang, 8753
1	MS9042	G. H. Evans, 8752
1	MS9042	S. K. Griffiths, 8752
1	MS9042	R. S. Larson, 8752

1	MS9042	C. D. Moen, 8752
1	MS9042	R. H. Nilson, 8752
1	MS9042	A. Ting, 8752
1	MS9403	L. A. Domeier, 8762
1	MS9403	B. E. Mills, 8773
1	MS9403	A. M. Morales, 8762
1	MS9403	N. Y. C. Yang, 8773
1	MS9405	K. L. Wilson, 8770
1	MS9409	J. R. Garcia, 8754
1	MS9409	S. H. Goods, 8754
1	MS9409	J. S. Korellis, 8754
1	MS9409	W.Y. Lu, 8754
3	MS9018	Central Technical Files, 8945-1
1	MS0899	Technical Library, 9616
1	MS9021	Classification Office, 8511, for Technical Library, MS0899, 9616
		DOE/OSTI via URL